

Eccentricity enables the earliest warning and localization of gravitational waves with ground-based detectors

Tao Yang^{1,2} Rong-Gen Cai^{3,4,5} Zhoujian Cao^{6,5,*} and Hyung Mok Lee²

¹*School of Physics and Technology, Wuhan University, Wuhan 430072, China*

²*Center for the Gravitational-Wave Universe, Astronomy Research Center, Seoul National University, 1 Gwanak-ro, Gwanak-gu, Seoul 08826, Korea*

³*CAS Key Laboratory of Theoretical Physics, Institute of Theoretical Physics, Chinese Academy of Sciences, Beijing 100190, China*

⁴*School of Physical Science and Technology, Ningbo University, Ningbo, 315211, China*

⁵*School of Fundamental Physics and Mathematical Sciences, Hangzhou Institute for Advanced Study (HIAS), University of Chinese Academy of Sciences, Hangzhou 310024, China*

⁶*Department of Astronomy, Beijing Normal University, Beijing 100875, China*

(Dated: May 15, 2024)

The early and precise localization of gravitational waves (GWs) is pivotal in detecting their electromagnetic (EM) counterparts, especially for binary neutron stars (BNS) and neutron star-black hole binaries (NSBH). In this letter, we pioneer the exploration of utilizing the higher harmonic modes induced by the eccentricity of compact binaries to localize GWs with ground-based detectors even before the quadrupole baseline $\ell = 2$ mode enters the detector band. Our theoretical analysis marks a first in proposing a strategy for gaining the earliest possible warning and maximizing preparation time for observing pre- and/or post-merger EM counterparts. We simulate three typical binaries from GWTC-3 with eccentricities ranging from 0.05 to 0.4. Our results reveal that the third-generation (3G) detectors (low frequency cut-off $f_0 = 5$ Hz) can accumulate sufficient signal-to-noise ratios through higher modes before the onset of the baseline $\ell = 2$ mode entry into the band. Notably, relying solely on the higher modes, the 3G detector network ET+2CE achieves an average localization on the order of $1 - 10^2 \text{ deg}^2$ around 1-1.8 hours before the merger of a GW170817-like BNS, and $10 - 10^3 \text{ deg}^2$ approximately 18-30 minutes prior to the merger of a GW200115-like NSBH. A 100 deg^2 localization is attainable even 2-4 hours prior to a BNS merger. Moreover, in the near face-on orientations which are generally more favorable for EM counterpart detection, the localization can be further improved.

I. INTRODUCTION

Multi-messenger observations of gravitational waves (GWs) and their electromagnetic (EM) counterparts play vital roles in cosmology, astrophysics, and fundamental physics [1–9]. Notably, with the observations of EM counterparts, the host galaxies of GWs and consequently their redshifts can be readily identified, enabling the direct measurement of the Hubble constant through GW standard sirens [3, 10–12] (for dark sirens with no EM counterparts see e.g. [13–19]). However, the successful capture of EM counterparts heavily relies on the precise and timely localization of GW sources [20–23]. The early warning and localization of GWs, as well as their implications for multi-messenger observations, have been explored from various perspectives [24–41].

Eccentricity can aid not only in distinguishing between isolated and dynamical binary black hole (BBH) formation scenarios [42–45] but also in improving the parameter estimation (including localization) of GWs [46–49]. In particular, recent studies [50–52] demonstrate that the eccentricity of long inspiraling compact binaries can dramatically enhance the accuracy of distance estimation and source localization by several orders of magnitude

with space-based decihertz observatories. On the other hand, neglecting eccentricity can introduce biases in parameter estimation and in testing general relativity with GWs [53–57]. In current detections, GW190521 has been suggested to favor nonzero eccentricities, and its effects on parameter estimation have been investigated from various perspectives [58–62]. These research findings suggest that eccentricity is an indispensable factor to consider in GW detection, data analysis, and practical applications.

One prominent feature of eccentric waveforms is the presence of multiple harmonic modes induced by eccentricity [63–66]. In the quasi-circular case, quadrupole GWs exhibit only the baseline mode, $\ell = 2$, whose frequency is twice of the orbital frequency F (hereafter, we refer to the $\ell = 2$ mode as the baseline mode). Eccentricity can induce higher harmonic modes, each with a frequency $f_\ell(t) = \ell F(t)$. This results in each mode entering the detector band at a distinct time. Consequently, the higher modes ($\ell > 2$) enter the detector band earlier than the dominant baseline mode, affording an extended period for the observation of these higher modes. This is particularly beneficial for ground-based detectors that aim to capture GWs at high frequencies, where the inspiral time is very limited. For instance, consider the binary neutron stars (BNS) GW170817 detected by LIGO as an example. The in-band time of the baseline mode from 10 Hz to the merger lasts approximately 17 minutes. However, before the baseline mode enters the detector band,

* Corresponding author: zjcao@bnu.edu.cn

the higher modes have already been in band for nearly 20 hours (assuming we account for the higher modes up to $\ell = 10$; note that a larger eccentricity would shorten this period). This extended observation window for the higher modes enables the consideration of Earth's rotation effects, introducing a Doppler effect that can furnish additional angular information regarding the sources. A nonvanishing eccentricity can render the contribution of these higher modes non-negligible even before the baseline mode becomes observable. The early detection and localization of these higher modes on their own have not been considered in previous works. This raises the following questions that we aim to address in this letter: Can we observe these higher modes even before the baseline mode becomes observable? More importantly, to what degree of accuracy can we localize GW sources solely based on these higher modes in the very early stage?

Previous works on the early warning of GWs have focused on the time following the entry of the dominant baseline mode into the band [25, 29, 30]. They aim at comparing the circular case (only baseline mode) to the eccentric case (baseline + higher modes) [25], or the quadrupole mode to the quadrupole + higher multipoles [29, 30]. In this letter, for the first time, we shift our focus to the time preceding the baseline dominant mode's entry. This means we exclusively rely on the higher modes in the very early stage. Localization based on these higher modes allows for the earliest detection and warning of GWs and electromagnetic (EM) counterparts, especially in the context of BNS and neutron star-black hole (NSBH) binaries. This grants EM telescopes much more preparation time, enhancing the likelihood of capturing EM counterparts and particularly aiding in the capture of potential pre-merger EM counterparts [67–70]. If there is a high likelihood that most NSBH mergers will involve non-disruptive systems, pre-merger signals might provide the sole avenue for EM observations of these systems.

II. METHODOLOGY

To address the aforementioned questions, we turn to simulations of typical compact binaries that have detected by LIGO-Virgo-KAGRA collaborations. We select three representative binaries from the GWTC-3 catalog [71]: BNS GW170817, NSBH GW200115, and binary black holes (BBH) GW150914. We consider various detector network scenarios, including the second-generation (2G) advanced LIGO, advanced Virgo, KAGRA, and India-LIGO (HLVKI) networks at their designed sensitivity, the third-generation (3G) detector Einstein Telescope (ET) [72], and the extended network ET+2CE, which combines ET with two cosmic explorer detectors¹. The

low-frequency cutoffs for the 2G and 3G detector bands are set at 10 Hz and 5 Hz, respectively. It's worth noting that the lower limit of ET can reach 3 Hz², which potentially yields more promising results. In this study, we conservatively assume a uniform lower limit of 5 Hz for all 3G detectors.

We adopt the non-spinning, inspiral-only, and frequency-domain EccentricFD waveform approximant provided by the LALSUITE software package [73]. This waveform is sufficient for our purposes, as we focus on the early stage of the inspiral phase. The eccentric waveforms are generated using PYCBC [74]. The waveform can be expressed as the sum of harmonics [64]:

$$\tilde{h}(f) = \sum_{\ell=1}^{10} \tilde{h}_{\ell}(f), \quad (1)$$

where $\tilde{h}_{\ell}(f)$ represents the contribution from the ℓ -th harmonic. We modify LALSUITE to extract each harmonic $\tilde{h}_{\ell}(f)$ separately.

Given the relationship $f_{\ell}(t) = \ell F(t)$, the time associated with a fixed frequency varies for each mode. Accounting for Earth's rotation, the antenna pattern functions $F_{+, \times}$ of the detector become time-dependent. Consequently, it's crucial to handle the antenna pattern function for each mode individually, ensuring accurate representation of their time-varying behavior. To establish the relationship between time and frequency $t(f)$ for eccentric binaries, we use the baseline frequency f_2 as a reference and numerically solve the phase evolution of the eccentric orbits [63]. Then for each mode $\tilde{h}_{\ell}(f)$, the associated response functions are $F_{+, \times}(t)$, with the time $t(f \rightarrow 2f/\ell)$. To assess the contribution of higher modes at a particular time, such as during the period before the baseline mode enters the band, each mode in Eq. (1) must be truncated at its respective frequency, which corresponds to the time when the baseline mode starts to enter the band.

We adopt the approach of [50] and employ the Fisher matrix technique for GWs [75] to estimate the uncertainty and covariance of the waveform parameters. The Fisher matrix is defined as $\Gamma_{ij} = (\partial_i h, \partial_j h)$, where $\partial_i h = \partial h / \partial P_i$ and P_i represents a parameter in the waveform (refer to [50, 51] for details). The inner product is defined as

$$(a, b) = 4 \int_{f_{\min}}^{f_{\max}} \frac{\tilde{a}^*(f)\tilde{b}(f) + \tilde{b}^*(f)\tilde{a}(f)}{2S_n(f)} df, \quad (2)$$

here f_{\min} is the low-frequency cutoff of the detector, $S_n(f)$ is the noise power spectral density. Then the signal-to-noise ratio (SNR) is $\rho = (h, h)$. The sky localization error is given by $\Delta\Omega = 2\pi |\sin(\theta)| \sqrt{C_{\theta\theta} C_{\phi\phi} - C_{\theta\phi}^2}$ [76], with the covariance matrix of the parameters as $C_{ij} = (\Gamma^{-1})_{ij}$. We need to note

¹ <https://gwic.ligo.org/>

² <https://apps.et-gw.eu/tds/?content=3&r=17196>

the limitations of the Fisher matrix in the parameter estimation of GWs, especially for low SNRs [77]. We incorporate Gaussian priors $\Gamma_{ii}^p = 1/(\delta P_i)^2$ into the Fisher information matrix, where δP_i represents the maximum permissible variation in the parameter [53, 54, 75, 78]. The Fisher matrix approach, with the incorporation of Gaussian priors, has demonstrated consistency with the more computationally intensive Markov Chain Monte Carlo (MCMC) method [54, 78].

To account for the different locations of the detectors and the effects of Earth's rotation, we use a geocentric coordinate system to derive the time-dependent antenna pattern functions of the detectors. Then, based on the relation $t(f)$ for each harmonic mode, we finally obtain the frequency-dependent antenna pattern functions (refer to [51, 52, 79] for the similar technical details). The positions and orientations of the arms for the 2G detector network HLVKI are detailed in Table I of [48]. However, the exact locations and orientations of the 3G detectors ET and CE have not been finalized. In our study, we assume ET is situated in the Netherlands, while the two CE detectors share the same locations and orientations as LIGO Hanford and Livingston³.

For each typical binary, we maintain the component masses (m_1 , m_2), redshift z , and luminosity distance d_L consistent with the median values of the actual events⁴. For angular parameters P_{ang} , such as the inclination angle ι , sky location (θ , ϕ), polarization angle ψ , and longitude of ascending nodes axis β , we generate 1000 random sets from a uniform and isotropic distribution. Given the validated use of this eccentric waveform for initial eccentricities up to 0.4 [64], we consider four discrete initial eccentricities: $e_0 = 0.05, 0.1, 0.2$, and 0.4 . It's important to note that e_0 is defined at $f_0 = 10$ Hz for 2G detectors and $f_0 = 5$ Hz for 3G detectors. Given that eccentricity is roughly inversely proportional to frequency [63], the same eccentricity value in the 3G detector context is more conservative than in the 2G detector scenario. Without loss of generality, we set the coalescence time and phase as $t_c = \phi_c = 0$.

III. RESULTS

Fig. 1 shows the average SNR and localization, provided exclusively by the higher modes ($\ell > 2$), just before the dominant baseline mode ($\ell = 2$) enters the band. We utilize two averaging strategies: first, by averaging across all 1000 P_{ang} samples, and second, by averaging the P_{ang} samples that meet the condition $|\cos \iota| \geq 0.9$. We define the condition $|\cos \iota| \geq 0.9$ (equivalently, $|\iota| \leq 25^\circ$ or $|180^\circ - \iota| \leq 25^\circ$) as near face-on orientations. These

orientations are optimal for achieving both a higher SNR and enhanced localization of the GWs. Furthermore, if we detect the EM counterparts of BNS and NSBH, they are more likely to be observed in near face-on orientations [80–82]. It's worth noting that the inclination angle of GW170817 was roughly 160° [3, 7, 83].

For the 2G detector network HLVKI, the average SNR from the higher modes, before the baseline mode enters the detector band, falls below the threshold SNR ρ_{th} in all cases. Only in near face-on orientations does the average SNR for BNS and BBH with $e_0 = 0.4$ meet the threshold. In contrast, all cases under the 3G detector scenarios not only surpass the SNR threshold but also achieve values on the order of 10^2 for BNS and BBH. This underscores that the 2G detector network lacks the requisite sensitivity to detect higher harmonic modes before the baseline mode enters the detector band. On the other hand, 3G detectors can amass a substantial SNR, enabling the easy detection of these higher modes.

For localization, we discard cases where the average localization exceeds 10^4 deg². In the HLVKI scenario, as expected, the early localization from the higher modes is poor and carries limited significance. However, the landscape changes dramatically with the 3G detectors. Using a single ET, the higher modes of BNS can secure an average localization that varies from 600 deg² at $e_0 = 0.05$ to 20 deg² at $e_0 = 0.4$, all before the baseline mode enters the band. Notably, in near face-on orientations, the localization is further enhanced, achieving an order of magnitude of $\mathcal{O}(1)$ deg² at $e_0 = 0.4$.

The inclusion of two CE detectors in conjunction with ET forms a network that can significantly enhance the localization of the higher modes. As depicted in the right panel of Fig. 1, the early localization solely from higher modes in nearly all cases is superior to 10^3 deg². For BNS, the average localization is 144.8, 34.5, 7.5, and 1.4 deg² for e_0 values of 0.05, 0.1, 0.2, and 0.4, respectively. In near face-on orientations, these localizations sharpen further to 38.5, 9.3, 2.0, and 0.34 deg², respectively. For NSBH, the average localization spans from 22.4 to 2477.8 deg² and refines to a range between 4.4 and 461.4 deg² in near face-on orientations. The results for BBH align closely in scale with those of BNS.

To assess how early the higher modes enable us to detect and localize the source, we show the evolution of average SNR and localization against time to merger for the three typical binaries within the ET+2CE network scenario in Fig. 2. We calculate the SNR and localization right before f_2 reaches 15 distinct values ranging from 1.5 to 50 Hz (note the baseline mode enters the band at $f_2 = 5$ Hz, so the results for this particular point just correspond to the right panel of Fig. 1). We then translate f_2 into the time to merger $t_c - t$, to obtain the evolution of SNR and localization against the time to merger. We place particular emphasis on the period preceding the entry of the baseline mode into the band. As illustrated in Fig. 2, in general, a larger eccentricity results in a higher SNR and better localization at a given

³ The exact detector location and orientation are not critical for this study and will not affect our results, as we simulate binaries uniformly distributed across the sky, aiming for average results.

⁴ <https://gwosc.org/eventapi/html/GWTC/>

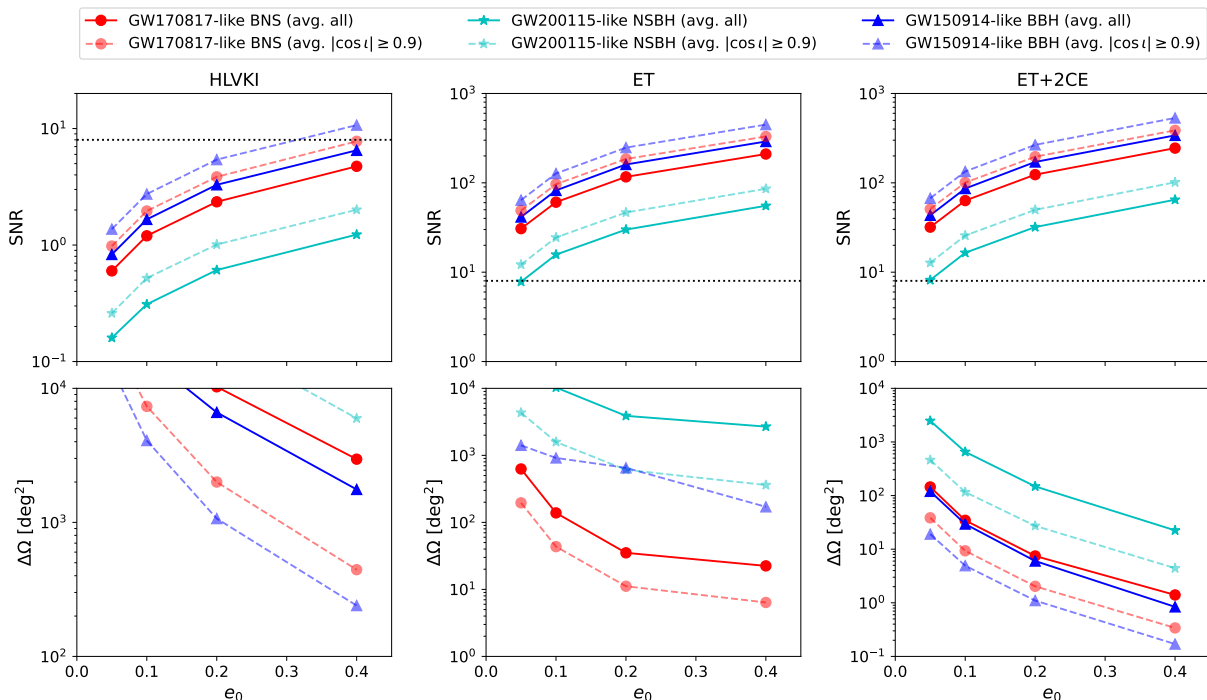


FIG. 1: The average SNR and localization provided exclusively by the higher harmonic modes just before the baseline mode enters the band. The luminosity distances for BNS, NSBH, and BBH are 40, 290, and 440 Mpc, respectively. The solid line represents the average of all 1000 P_{ang} samples, while the dashed line corresponds to the average with $|\cos \iota| \geq 0.9$ (near face-on orientations). The dotted lines in the upper panel indicate the threshold SNR, $\rho_{\text{th}} = 8$. Only cases with $\Delta\Omega < 10^4 \text{ deg}^2$ are shown.

time. For BNS, with eccentricities ranging from 0.05 to 0.4, the higher modes can achieve the threshold SNR between 4.5 to 7.5 hours prior to the merger. This is notably earlier than the entry of the baseline mode into the band. Localization of 100 deg^2 can be achieved around 2-4 hours prior to the merger, derived solely from the higher modes before the quadrupole mode's entry into the band (except for $e_0 = 0.05$, which is slightly after the baseline mode enters the band). In the case of NSBH, the threshold SNR can be obtained 0.5-1.3 hours before the merger. Solely relying on the higher modes, a localization of 100 deg^2 can be achieved 30 minutes before the merger when $e_0 = 0.4$. The results of BBH are similar to that of BNS, though with a significantly shorter time to merger: 1.3-2.2 minutes for the threshold SNR and 30-50 seconds for a 100 deg^2 localization. In near face-on orientations, the results above can be further improved.

IV. DISCUSSION

In this letter, we aim at checking the idea that whether the higher harmonic modes of eccentric compact binaries can make a significant contribution to the SNR and localization of the sources, even before the dominant baseline mode enters the detector band. Consequently, these higher modes could offer the earliest alert and localiza-

tion, thereby optimizing preparation time for both pre- and post-merger EM counterpart observations. Our findings hold significance not only for the EM counterpart observations of BNS and NSBH but also for the potential EM follow-ups of BBH [84–86].

We fixed the distances of the three typical binaries to match the median values of the true events. However, our methodology can easily be extended to other distances, as there is a relationship in our calculation of SNR and localization: $\rho \sim 1/d_L$ and $\Delta\Omega \sim 1/\rho^2 \sim d_L^2$.

The rate of eccentric binaries remains a topic of active research [87–90]. These estimates crucially depend on the unknown astrophysics of these classes of compact binaries. For BNS, which are the most promising and sought-after early warning candidates, the rate of eccentric events could be rare [87]. However, the detection of even a single such event would be highly significant. The methodology proposed in our paper could provide the maximum preparation time for observations, thereby significantly increasing the likelihood of successful joint GW and EM observations. Given the extreme rarity of EM counterparts in current GW detections, a very early warning of a potential GW + EM signal could be of great interest to both the GW community and EM follow-up teams. Our approach offers a promising avenue to enhance the detection and understanding of these rare and valuable events.

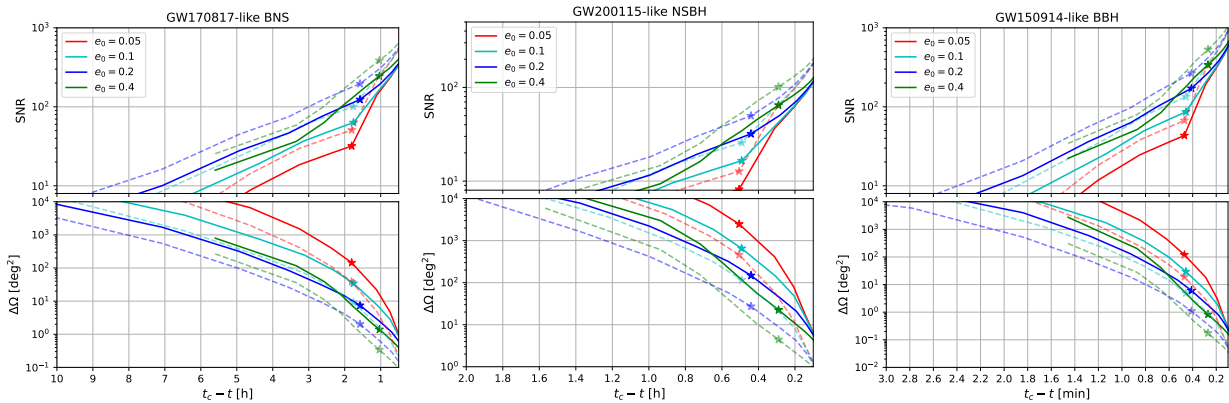


FIG. 2: The average SNR and localization that can be achieved before the time to merger in the ET+2CE scenario.

The luminosity distances for BNS, NSBH, and BBH are 40, 290, and 440 Mpc, respectively. The solid line represents the average of all 1000 P_{ang} samples, while the dashed line corresponds to the average with $|\cos i| \geq 0.9$ (near face-on orientations). Stars indicate $f_2 = 5$ Hz, marking the point where the dominant baseline mode begins to enter the band.

ACKNOWLEDGMENTS

This work is supported by the National Research Foundation of Korea 2021R1A2C2012473 and 2021M3F7A1082056. T. Y. is supported by “the Fundamental Research Funds for the Central Universities” under the reference No. 2042024FG0009. R.G.C. is supported by the National Key Research and Development Program of China Grant No. 2020YFC2201502 and

2021YFA0718304 and by National Natural Science Foundation of China Grants No. 11821505, No. 11991052, No. 11947302, No. 12235019. Z.C. is supported in part by the National Key Research and Development Program of China Grant No. 2021YFC2203001, in part by the NSFC (No. 11920101003 and No. 12021003), in part by “the Interdisciplinary Research Funds of Beijing Normal University” and in part by CAS Project for Young Scientists in Basic Research YSBR-006.

-
- [1] B. P. Abbott *et al.* (LIGO Scientific, Virgo, Fermi GBM, INTEGRAL, IceCube, AstroSat Cadmium Zinc Telluride Imager Team, IPN, Insight-Hxmt, ANTARES, Swift, AGILE Team, 1M2H Team, Dark Energy Camera GW-EM, DES, DLT40, GRAWITA, Fermi-LAT, ATCA, ASKAP, Las Cumbres Observatory Group, OzGrav, DWF (Deeper Wider Faster Program), AST3, CAAS-TRO, VINROUGE, MASTER, J-GEM, GROWTH, JAGWAR, CaltechNRAO, TTU-NRAO, NuSTAR, Pan-STARRS, MAXI Team, TZAC Consortium, KU, Nordic Optical Telescope, ePESSTO, GROND, Texas Tech University, SALT Group, TOROS, BOOTES, MWA, CALET, IKI-GW Follow-up, H.E.S.S., LOFAR, LWA, HAWC, Pierre Auger, ALMA, Euro VLBI Team, Pi of Sky, Chandra Team at McGill University, DFN, ATLAS Telescopes, High Time Resolution Universe Survey, RIMAS, RATIR, SKA South Africa/MeerKAT), Multi-messenger Observations of a Binary Neutron Star Merger, *Astrophys. J. Lett.* **848**, L12 (2017), [arXiv:1710.05833 \[astro-ph.HE\]](#).
- [2] B. P. Abbott *et al.* (LIGO Scientific, Virgo, Fermi-GBM, INTEGRAL), Gravitational Waves and Gamma-rays from a Binary Neutron Star Merger: GW170817 and GRB 170817A, *Astrophys. J. Lett.* **848**, L13 (2017), [arXiv:1710.05834 \[astro-ph.HE\]](#).
- [3] B. P. Abbott *et al.* (LIGO Scientific, Virgo, 1M2H, Dark Energy Camera GW-E, DES, DLT40, Las Cumbres Observatory, VINROUGE, MASTER), A gravitational-wave standard siren measurement of the Hubble constant, *Nature* **551**, 85 (2017), [arXiv:1710.05835 \[astro-ph.CO\]](#).
- [4] P. Creminelli and F. Vernizzi, Dark Energy after GW170817 and GRB170817A, *Phys. Rev. Lett.* **119**, 251302 (2017), [arXiv:1710.05877 \[astro-ph.CO\]](#).
- [5] J. M. Ezquiaga and M. Zumalacárregui, Dark Energy After GW170817: Dead Ends and the Road Ahead, *Phys. Rev. Lett.* **119**, 251304 (2017), [arXiv:1710.05901 \[astro-ph.CO\]](#).
- [6] T. Baker, E. Bellini, P. G. Ferreira, M. Lagos, J. Noller, and I. Sawicki, Strong constraints on cosmological gravity from GW170817 and GRB 170817A, *Phys. Rev. Lett.* **119**, 251301 (2017), [arXiv:1710.06394 \[astro-ph.CO\]](#).
- [7] K. P. Mooley, A. T. Deller, O. Gottlieb, E. Nakar, G. Hallinan, S. Bourke, D. A. Frail, A. Horesh, A. Corsi, and K. Hotokezaka, Superluminal motion of a relativistic jet in the neutron-star merger GW170817, *Nature* **561**, 355 (2018), [arXiv:1806.09693 \[astro-ph.HE\]](#).
- [8] K. Hotokezaka, E. Nakar, O. Gottlieb, S. Nissanke, K. Masuda, G. Hallinan, K. P. Mooley, and A. T. Deller, A Hubble constant measurement from superluminal motion of the jet in GW170817, *Nature Astron.* **3**, 940 (2019), [arXiv:1806.10596 \[astro-ph.CO\]](#).

- [9] T. Dietrich, M. W. Coughlin, P. T. H. Pang, M. Bulla, J. Heinzl, L. Issa, I. Tews, and S. Antier, Multimes-senger constraints on the neutron-star equation of state and the Hubble constant, *Science* **370**, 1450 (2020), [arXiv:2002.11355 \[astro-ph.HE\]](#).
- [10] D. E. Holz and S. A. Hughes, Using gravitational-wave standard sirens, *Astrophys. J.* **629**, 15 (2005), [arXiv:astro-ph/0504616](#).
- [11] N. Dalal, D. E. Holz, S. A. Hughes, and B. Jain, Short grb and binary black hole standard sirens as a probe of dark energy, *Phys. Rev. D* **74**, 063006 (2006), [arXiv:astro-ph/0601275](#).
- [12] S. Nissanke, D. E. Holz, S. A. Hughes, N. Dalal, and J. L. Sievers, Exploring short gamma-ray bursts as gravitational-wave standard sirens, *Astrophys. J.* **725**, 496 (2010), [arXiv:0904.1017 \[astro-ph.CO\]](#).
- [13] H.-Y. Chen, M. Fishbach, and D. E. Holz, A two per cent Hubble constant measurement from standard sirens within five years, *Nature* **562**, 545 (2018), [arXiv:1712.06531 \[astro-ph.CO\]](#).
- [14] S. Borhanian, A. Dhani, A. Gupta, K. G. Arun, and B. S. Sathyaprakash, Dark Sirens to Resolve the Hubble–Lemaître Tension, *Astrophys. J. Lett.* **905**, L28 (2020), [arXiv:2007.02883 \[astro-ph.CO\]](#).
- [15] M. Fishbach *et al.* (LIGO Scientific, Virgo), A Standard Siren Measurement of the Hubble Constant from GW170817 without the Electromagnetic Counterpart, *Astrophys. J. Lett.* **871**, L13 (2019), [arXiv:1807.05667 \[astro-ph.CO\]](#).
- [16] M. Soares-Santos *et al.* (DES, LIGO Scientific, Virgo), First Measurement of the Hubble Constant from a Dark Standard Siren using the Dark Energy Survey Galaxies and the LIGO/Virgo Binary–Black-hole Merger GW170814, *Astrophys. J. Lett.* **876**, L7 (2019), [arXiv:1901.01540 \[astro-ph.CO\]](#).
- [17] R. Gray *et al.*, Cosmological inference using gravitational wave standard sirens: A mock data analysis, *Phys. Rev. D* **101**, 122001 (2020), [arXiv:1908.06050 \[gr-qc\]](#).
- [18] A. Palmese *et al.* (DES), A statistical standard siren measurement of the Hubble constant from the LIGO/Virgo gravitational wave compact object merger GW190814 and Dark Energy Survey galaxies, *Astrophys. J. Lett.* **900**, L33 (2020), [arXiv:2006.14961 \[astro-ph.CO\]](#).
- [19] A. Finke, S. Foffa, F. Iacovelli, M. Maggiore, and M. Mancarella, Cosmology with LIGO/Virgo dark sirens: Hubble parameter and modified gravitational wave propagation, *JCAP* **08**, 026, [arXiv:2101.12660 \[astro-ph.CO\]](#).
- [20] P. Petrov, L. P. Singer, M. W. Coughlin, V. Kumar, M. Almualla, S. Anand, M. Bulla, T. Dietrich, F. Foucart, and N. Guessoum, Data-driven Expectations for Electromagnetic Counterpart Searches Based on LIGO/Virgo Public Alerts, *Astrophys. J.* **924**, 54 (2022), [arXiv:2108.07277 \[astro-ph.HE\]](#).
- [21] Q. Chu, E. J. Howell, A. Rowlinson, H. Gao, B. Zhang, S. J. Tingay, M. Boër, and L. Wen, Capturing the electromagnetic counterparts of binary neutron star mergers through low latency gravitational wave triggers, *Mon. Not. Roy. Astron. Soc.* **459**, 121 (2016), [arXiv:1509.06876 \[astro-ph.HE\]](#).
- [22] S. Ghosh, S. Bloemen, G. Nelemans, P. J. Groot, and L. R. Price, Tiling strategies for optical follow-up of gravitational-wave triggers by telescopes with a wide field of view, *Astron. Astrophys.* **592**, A82 (2016), [arXiv:1511.02673 \[astro-ph.IM\]](#).
- [23] M. W. Coughlin *et al.*, Optimizing searches for electromagnetic counterparts of gravitational wave triggers, *Mon. Not. Roy. Astron. Soc.* **478**, 692 (2018), [arXiv:1803.02255 \[astro-ph.IM\]](#).
- [24] K. Cannon *et al.*, Toward Early-Warning Detection of Gravitational Waves from Compact Binary Coalescence, *Astrophys. J.* **748**, 136 (2012), [arXiv:1107.2665 \[astro-ph.IM\]](#).
- [25] K. Kyutoku and N. Seto, Pre-merger localization of eccentric compact binary coalescences with second-generation gravitational-wave detector networks, *Mon. Not. Roy. Astron. Soc.* **441**, 1934 (2014), [arXiv:1312.2953 \[astro-ph.HE\]](#).
- [26] M. L. Chan, C. Messenger, I. S. Heng, and M. Hendry, Binary Neutron Star Mergers and Third Generation Detectors: Localization and Early Warning, *Phys. Rev. D* **97**, 123014 (2018), [arXiv:1803.09680 \[astro-ph.HE\]](#).
- [27] A. H. Nitz, M. Schäfer, and T. Dal Canton, Gravitational-wave Merger Forecasting: Scenarios for the Early Detection and Localization of Compact-binary Mergers with Ground-based Observatories, *Astrophys. J. Lett.* **902**, L29 (2020), [arXiv:2009.04439 \[astro-ph.HE\]](#).
- [28] M. K. Singh, S. J. Kapadia, M. A. Shaikh, D. Chatterjee, and P. Ajith, Improved early warning of compact binary mergers using higher modes of gravitational radiation: A population study, *Mon. Not. Roy. Astron. Soc.* **502**, 1612 (2021), [arXiv:2010.12407 \[astro-ph.HE\]](#).
- [29] S. J. Kapadia, M. K. Singh, M. A. Shaikh, D. Chatterjee, and P. Ajith, Of Harbingers and Higher Modes: Improved gravitational-wave early-warning of compact binary mergers, *Astrophys. J. Lett.* **898**, L39 (2020), [arXiv:2005.08830 \[astro-ph.HE\]](#).
- [30] M. K. Singh, D. Divyajyoti, S. J. Kapadia, M. A. Shaikh, and P. Ajith, Improved early-warning estimates of luminosity distance and orbital inclination of compact binary mergers using higher modes of gravitational radiation, *Mon. Not. Roy. Astron. Soc.* **513**, 3798 (2022), [arXiv:2202.05802 \[astro-ph.HE\]](#).
- [31] T. Tsutsui, A. Nishizawa, and S. Morisaki, Early warning of precessing compact binary merger with third-generation gravitational-wave detectors, *Phys. Rev. D* **104**, 064013 (2021), [arXiv:2011.06130 \[gr-qc\]](#).
- [32] R. Magee *et al.*, First demonstration of early warning gravitational wave alerts, *Astrophys. J. Lett.* **910**, L21 (2021), [arXiv:2102.04555 \[astro-ph.HE\]](#).
- [33] R. Magee and S. Borhanian, Observing Scenarios for the Next Decade of Early Warning Detection of Binary Neutron Stars, *Astrophys. J.* **935**, 139 (2022), [arXiv:2201.11841 \[astro-ph.HE\]](#).
- [34] T. Tsutsui, A. Nishizawa, and S. Morisaki, Early warning of precessing neutron-star black hole binary mergers with the near-future gravitational-wave detectors, *Mon. Not. Roy. Astron. Soc.* **512**, 3878 (2022), [arXiv:2107.12531 \[gr-qc\]](#).
- [35] C. Chatterjee and L. Wen, Pre-merger sky localization of gravitational waves from binary neutron star mergers using deep learning, (2022), [arXiv:2301.03558 \[astro-ph.HE\]](#).
- [36] Y. Li, I. S. Heng, M. L. Chan, C. Messenger, and X. Fan, Exploring the sky localization and early warning capabilities of third generation gravitational wave detectors in three-detector network configurations, *Phys. Rev. D* **105**, 043010 (2022), [arXiv:2109.07389 \[astro-ph.IM\]](#).
- [37] A. L. Miller, N. Singh, and C. Palomba, Enabling

- multi-messenger astronomy with continuous gravitational waves: early warning and sky localization of binary neutron stars in Einstein Telescope, (2023), [arXiv:2309.15808 \[astro-ph.IM\]](#).
- [38] S. Sachdev *et al.*, An Early-warning System for Electromagnetic Follow-up of Gravitational-wave Events, *Astrophys. J. Lett.* **905**, L25 (2020), [arXiv:2008.04288 \[astro-ph.HE\]](#).
- [39] M. Kovalam, M. A. K. Patwary, A. K. Sreekumar, L. Wen, F. H. Panther, and Q. Chu, Early Warnings of Binary Neutron Star Coalescence Using the SPIIR Search, *Astrophys. J. Lett.* **927**, L9 (2022), [arXiv:2112.03597 \[gr-qc\]](#).
- [40] S. S. Chaudhary *et al.*, Low-latency gravitational wave alert products and their performance in anticipation of the fourth LIGO-Virgo-KAGRA observing run, (2023), [arXiv:2308.04545 \[astro-ph.HE\]](#).
- [41] Q. Hu and J. Veitch, Rapid Premerger Localization of Binary Neutron Stars in Third-generation Gravitational-wave Detectors, *Astrophys. J. Lett.* **958**, L43 (2023), [arXiv:2309.00970 \[gr-qc\]](#).
- [42] A. Nishizawa, E. Berti, A. Klein, and A. Sesana, eLISA eccentricity measurements as tracers of binary black hole formation, *Phys. Rev. D* **94**, 064020 (2016), [arXiv:1605.01341 \[gr-qc\]](#).
- [43] A. Nishizawa, A. Sesana, E. Berti, and A. Klein, Constraining stellar binary black hole formation scenarios with eLISA eccentricity measurements, *Mon. Not. Roy. Astron. Soc.* **465**, 4375 (2017), [arXiv:1606.09295 \[astro-ph.HE\]](#).
- [44] K. Breivik, C. L. Rodriguez, S. L. Larson, V. Kalogera, and F. A. Rasio, Distinguishing Between Formation Channels for Binary Black Holes with LISA, *Astrophys. J. Lett.* **830**, L18 (2016), [arXiv:1606.09558 \[astro-ph.GA\]](#).
- [45] M. Zevin, I. M. Romero-Shaw, K. Kremer, E. Thrane, and P. D. Lasky, Implications of Eccentric Observations on Binary Black Hole Formation Channels, *Astrophys. J. Lett.* **921**, L43 (2021), [arXiv:2106.09042 \[astro-ph.HE\]](#).
- [46] B. Sun, Z. Cao, Y. Wang, and H.-C. Yeh, Parameter estimation of eccentric inspiraling compact binaries using an enhanced post circular model for ground-based detectors, *Phys. Rev. D* **92**, 044034 (2015).
- [47] S. Ma, Z. Cao, C.-Y. Lin, H.-P. Pan, and H.-J. Yo, Gravitational wave source localization for eccentric binary coalesce with a ground-based detector network, *Phys. Rev. D* **96**, 084046 (2017), [arXiv:1710.02965 \[gr-qc\]](#).
- [48] H.-P. Pan, C.-Y. Lin, Z. Cao, and H.-J. Yo, Accuracy of source localization for eccentric inspiraling binary mergers using a ground-based detector network, *Phys. Rev. D* **100**, 124003 (2019), [arXiv:1912.04455 \[gr-qc\]](#).
- [49] B. Mikoczi, B. Kocsis, P. Forgacs, and M. Vasuth, Parameter estimation for inspiraling eccentric compact binaries including pericenter precession, *Phys. Rev. D* **86**, 104027 (2012), [arXiv:1206.5786 \[gr-qc\]](#).
- [50] T. Yang, R.-G. Cai, Z. Cao, and H. M. Lee, Eccentricity of Long Inspiring Compact Binaries Sheds Light on Dark Sirens, *Phys. Rev. Lett.* **129**, 191102 (2022), [arXiv:2202.08608 \[gr-qc\]](#).
- [51] T. Yang, R.-G. Cai, Z. Cao, and H. M. Lee, Parameter estimation of eccentric gravitational waves with a decihertz observatory and its cosmological implications, *Phys. Rev. D* **107**, 043539 (2023), [arXiv:2212.11131 \[gr-qc\]](#).
- [52] T. Yang, R.-G. Cai, and H. M. Lee, Space-borne atom interferometric gravitational wave detections. Part III. Eccentricity on dark sirens, *JCAP* **10**, 061, [arXiv:2208.10998 \[gr-qc\]](#).
- [53] M. Favata, Systematic parameter errors in inspiraling neutron star binaries, *Phys. Rev. Lett.* **112**, 101101 (2014), [arXiv:1310.8288 \[gr-qc\]](#).
- [54] M. Favata, C. Kim, K. G. Arun, J. Kim, and H. W. Lee, Constraining the orbital eccentricity of inspiralling compact binary systems with Advanced LIGO, *Phys. Rev. D* **105**, 023003 (2022), [arXiv:2108.05861 \[gr-qc\]](#).
- [55] H. Gil Choi, T. Yang, and H. M. Lee, Importance of Eccentricities in Parameter Estimation of Compact Binary Inspirals with Decihertz Gravitational-Wave Detectors, (2022), [arXiv:2210.09541 \[gr-qc\]](#).
- [56] P. Saini, M. Favata, and K. G. Arun, Systematic bias on parametrized tests of general relativity due to neglect of orbital eccentricity, *Phys. Rev. D* **106**, 084031 (2022), [arXiv:2203.04634 \[gr-qc\]](#).
- [57] P. Narayan, N. K. Johnson-McDaniel, and A. Gupta, Effect of ignoring eccentricity in testing general relativity with gravitational waves, *Phys. Rev. D* **108**, 064003 (2023), [arXiv:2306.04068 \[gr-qc\]](#).
- [58] I. M. Romero-Shaw, P. D. Lasky, E. Thrane, and J. C. Bustillo, GW190521: orbital eccentricity and signatures of dynamical formation in a binary black hole merger signal, *Astrophys. J. Lett.* **903**, L5 (2020), [arXiv:2009.04771 \[astro-ph.HE\]](#).
- [59] V. Gayathri, J. Healy, J. Lange, B. O'Brien, M. Szczepanczyk, I. Bartos, M. Campanelli, S. Klimentko, C. O. Lousto, and R. O'Shaughnessy, Eccentricity estimate for black hole mergers with numerical relativity simulations, *Nature Astron.* **6**, 344 (2022), [arXiv:2009.05461 \[astro-ph.HE\]](#).
- [60] V. Gayathri, J. Healy, J. Lange, B. O'Brien, M. Szczepanczyk, I. Bartos, M. Campanelli, S. Klimentko, C. O. Lousto, and R. O'Shaughnessy, Measuring the Hubble Constant with GW190521 as an Eccentric black hole Merger and Its Potential Electromagnetic Counterpart, *Astrophys. J. Lett.* **908**, L34 (2021), [arXiv:2009.14247 \[astro-ph.HE\]](#).
- [61] R. Abbott *et al.* (LIGO Scientific, Virgo), Properties and Astrophysical Implications of the $150 M_{\odot}$ Binary Black Hole Merger GW190521, *Astrophys. J. Lett.* **900**, L13 (2020), [arXiv:2009.01190 \[astro-ph.HE\]](#).
- [62] R. Abbott *et al.* (LIGO Scientific, Virgo), GW190521: A Binary Black Hole Merger with a Total Mass of $150 M_{\odot}$, *Phys. Rev. Lett.* **125**, 101102 (2020), [arXiv:2009.01075 \[gr-qc\]](#).
- [63] N. Yunes, K. G. Arun, E. Berti, and C. M. Will, Post-Circular Expansion of Eccentric Binary Inspirals: Fourier-Domain Waveforms in the Stationary Phase Approximation, *Phys. Rev. D* **80**, 084001 (2009), [Erratum: *Phys. Rev. D* **89**, 109901 (2014)], [arXiv:0906.0313 \[gr-qc\]](#).
- [64] E. A. Huerta, P. Kumar, S. T. McWilliams, R. O'Shaughnessy, and N. Yunes, Accurate and efficient waveforms for compact binaries on eccentric orbits, *Phys. Rev. D* **90**, 084016 (2014), [arXiv:1408.3406 \[gr-qc\]](#).
- [65] B. Moore, T. Robson, N. Loutrel, and N. Yunes, Towards a Fourier domain waveform for non-spinning binaries with arbitrary eccentricity, *Class. Quant. Grav.* **35**, 235006 (2018), [arXiv:1807.07163 \[gr-qc\]](#).
- [66] B. Moore and N. Yunes, A 3PN Fourier Domain Waveform for Non-Spinning Binaries with Moderate

- Eccentricity, *Class. Quant. Grav.* **36**, 185003 (2019), [arXiv:1903.05203 \[gr-qc\]](#).
- [67] D. Tsang, J. S. Read, T. Hinderer, A. L. Piro, and R. Bondarescu, Resonant Shattering of Neutron Star Crusts, *Phys. Rev. Lett.* **108**, 011102 (2012), [arXiv:1110.0467 \[astro-ph.HE\]](#).
- [68] A. G. Suvorov and K. D. Kokkotas, Precursor flares of short gamma-ray bursts from crust yielding due to tidal resonances in coalescing binaries of rotating, magnetized neutron stars, *Phys. Rev. D* **101**, 083002 (2020), [arXiv:2003.05673 \[astro-ph.HE\]](#).
- [69] M. Lyutikov, Electrodynamics of binary neutron star mergers, *Mon. Not. Roy. Astron. Soc.* **483**, 2766 (2019), [arXiv:1809.10478 \[astro-ph.HE\]](#).
- [70] V. Paschalidis, Z. B. Etienne, and S. L. Shapiro, General relativistic simulations of binary black hole-neutron stars: Precursor electromagnetic signals, *Phys. Rev. D* **88**, 021504 (2013), [arXiv:1304.1805 \[astro-ph.HE\]](#).
- [71] R. Abbott *et al.* (LIGO Scientific, VIRGO, KAGRA), GWTC-3: Compact Binary Coalescences Observed by LIGO and Virgo During the Second Part of the Third Observing Run, (2021), [arXiv:2111.03606 \[gr-qc\]](#).
- [72] M. Punturo *et al.*, The Einstein Telescope: A third-generation gravitational wave observatory, *Class. Quant. Grav.* **27**, 194002 (2010).
- [73] LIGO Scientific Collaboration, *LIGO Algorithm Library - LALSuite*, free software (GPL) (2018).
- [74] A. Nitz, I. Harry, D. Brown, C. M. Biwer, J. Willis, T. D. Canton, C. Capano, T. Dent, L. Pekowsky, A. R. Williamson, S. De, M. Cabero, B. Machenschalk, D. Macleod, P. Kumar, F. Pannarale, S. Reyes, G. S. C. Davies, dfinstad, S. Kumar, M. Tápai, L. Singer, S. Khan, S. Fairhurst, A. Nielsen, S. Singh, T. Massinger, K. Chandra, shasvath, and veronica villa, *gwastro/pycbc: v2.0.5 release of pycbc* (2022).
- [75] C. Cutler and E. E. Flanagan, Gravitational waves from merging compact binaries: How accurately can one extract the binary's parameters from the inspiral wave form?, *Phys. Rev. D* **49**, 2658 (1994), [arXiv:gr-qc/9402014](#).
- [76] C. Cutler, Angular resolution of the LISA gravitational wave detector, *Phys. Rev. D* **57**, 7089 (1998), [arXiv:gr-qc/9703068](#).
- [77] M. Vallisneri, Use and abuse of the Fisher information matrix in the assessment of gravitational-wave parameter-estimation prospects, *Phys. Rev. D* **77**, 042001 (2008), [arXiv:gr-qc/0703086](#).
- [78] H.-S. Cho, Systematic bias due to eccentricity in parameter estimation for merging binary neutron stars, *Phys. Rev. D* **105**, 124022 (2022), [arXiv:2205.12531 \[gr-qc\]](#).
- [79] P. W. Graham and S. Jung, Localizing Gravitational Wave Sources with Single-Baseline Atom Interferometers, *Phys. Rev. D* **97**, 024052 (2018), [arXiv:1710.03269 \[gr-qc\]](#).
- [80] A. A. Abdo *et al.* (Fermi-LAT, Fermi GBM), Fermi Observations of High-Energy Gamma-Ray Emission from GRB 080916C, *Science* **323**, 1688 (2009).
- [81] E. Nakar, A. Gal-Yam, and D. B. Fox, The Local Rate and the Progenitor Lifetimes of Short-Hard Gamma-Ray Bursts: Synthesis and Predictions for LIGO, *Astrophys. J.* **650**, 281 (2006), [arXiv:astro-ph/0511254](#).
- [82] L. Rezzolla, B. Giacomazzo, L. Baiotti, J. Granot, C. Kouveliotou, and M. A. Aloy, The missing link: Merging neutron stars naturally produce jet-like structures and can power short Gamma-Ray Bursts, *Astrophys. J. Lett.* **732**, L6 (2011), [arXiv:1101.4298 \[astro-ph.HE\]](#).
- [83] K. P. Mooley, J. Anderson, and W. Lu, Optical superluminal motion measurement in the neutron-star merger GW170817, *Nature* **610**, 273 (2022), [arXiv:2210.06568 \[astro-ph.HE\]](#).
- [84] V. Connaughton *et al.*, Fermi GBM Observations of LIGO Gravitational Wave event GW150914, *Astrophys. J. Lett.* **826**, L6 (2016), [arXiv:1602.03920 \[astro-ph.HE\]](#).
- [85] A. Loeb, Electromagnetic Counterparts to Black Hole Mergers Detected by LIGO, *Astrophys. J. Lett.* **819**, L21 (2016), [arXiv:1602.04735 \[astro-ph.HE\]](#).
- [86] S. E. d. Mink and A. King, Electromagnetic signals following stellar-mass black hole mergers, *Astrophys. J. Lett.* **839**, L7 (2017), [arXiv:1703.07794 \[astro-ph.HE\]](#).
- [87] C. S. Ye, W.-f. Fong, K. Kremer, C. L. Rodriguez, S. Chatterjee, G. Fragione, and F. A. Rasio, On the Rate of Neutron Star Binary Mergers from Globular Clusters, *Astrophys. J. Lett.* **888**, L10 (2020), [arXiv:1910.10740 \[astro-ph.HE\]](#).
- [88] J. Samsing, M. MacLeod, and E. Ramirez-Ruiz, The Formation of Eccentric Compact Binary Inspirals and the Role of Gravitational Wave Emission in Binary-Single Stellar Encounters, *Astrophys. J.* **784**, 71 (2014), [arXiv:1308.2964 \[astro-ph.HE\]](#).
- [89] J. Samsing, Eccentric Black Hole Mergers Forming in Globular Clusters, *Phys. Rev. D* **97**, 103014 (2018), [arXiv:1711.07452 \[astro-ph.HE\]](#).
- [90] J. Samsing and E. Ramirez-Ruiz, On the Assembly Rate of Highly Eccentric Binary Black Hole Mergers, *Astrophys. J. Lett.* **840**, L14 (2017), [arXiv:1703.09703 \[astro-ph.HE\]](#).